Inorganic Chemistry

Article

pubs.acs.org/IC

$Pb_4V_6O_{16}(SeO_3)_3(H_2O)$, $Pb_2VO_2(SeO_3)_2Cl$, and $PbVO_2(SeO_3)F$: New Lead(II)−Vanadium(V) Mixed-Metal Selenites Featuring Novel Anionic Skeletons

Xue-Li Cao,[†,‡] Fang Kong,[†] Chun-Li Hu,[†] Xiang Xu,[†] and Jiang-Gao Mao*[,†]

[†]State Key Laboratory of Structural Chemistry, Fujian Institute of Research on the Structure of Matter, Chinese Academy of Sciences, Fuzhou 350002, People's Republic of China

[‡]University of the Chinese Academy of Sciences, Beijing 100039, People's Republic of China

Supporting Information

ABSTRACT: Hydrothermal reactions of $PbCO_3$ (or $PbCl_2$), V_2O_5, and SeO_2 in KOH solution or HF solution resulted in three new lead(II)−vanadium(V) mixed-metal selenites, namely, $Pb_4V_6O_{16}(SeO_3)_3(H_2O)$ (**1**), $Pb_2VO_2(SeO_3)_2Cl$ (**2**), and $PbVO_2(SeO_3)F$ (**3**). Compounds **1** and **2** are polar (space group $P2_1$), whereas compound **3** is centrosymmetric (space group *Pbca*). Compound **1** displays an unusual $[V_6O_{16}(SeO_3)_3]^{8-}$ anionic chain, which is composed by a 1D $[V_4O_{12}]^{2-}$ anionic chain that is further decorated by dimeric $[V_2O_6(SeO_3)_3]^{8-}$ units via corner-sharing. Compound **2** features two types of 1D chains, a cationic $[Pb_2Cl]^{3+}$ chain and a $[VO_2(SeO_3)_2]^{3-}$ anionic chain, whereas compound **3** contains dimeric $[V_2O_4(SeO_3)_2F_2]^{2-}$ units. The powder second-harmonic-generating (SHG) measurements indicate that compound **1** shows a weak SHG response of about 0.2 × KDP (KH_2PO_4) under 1400 nm laser radiation. Thermal stability and optical properties as well as theoretical calculations based on density functional theory methods were also performed.

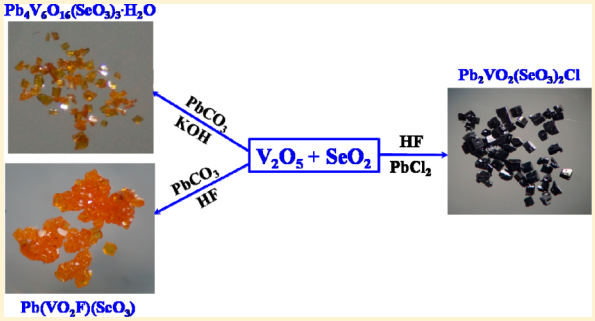

INTRODUCTION

During the last two decades, metal selenites and tellurites have received a lot of research attention from scientists in inorganic chemistry and materials chemistry. The presence of the active lone-pair electrons of Se^{4+} and Te^{4+} cations, which are susceptible to second-order Jahn−Teller (SOJT) distortions, can serve as a structure-directing agent and aid in the formation of noncentrosymmetric (NCS) structures with possible second-harmonic generation (SHG).[1,2] So far, a large number of SHG materials based on metal selenites or tellurites have been synthesized, including $TeSeO_4$, Te_2SeO_7, and $B_2Se_2O_7$.[3a,4e,5] Research also indicates that the introduction of octahedrally coordinated transition metal (TM) ions with d^0 electronic configuration such as V^{5+} (Ti^{4+}, Nb^{5+}, Mo^{6+}, W^{6+}, Ta^{5+}), and counter-cations with lone-pair electrons such as Pb^{2+} and Bi^{3+}, into the metal selenite and tellurite systems is also an effective synthetic route for designing new noncentrosymmetric structures.[3,4b,6] As for the Pb^{2+}-d^0-TM-Se^{4+}-O system, seven compounds have been reported, namely, $Pb_2V_2Se_2O_{11}$, $Pb_2V_3Se_5O_{18}$, $Pb_4(VO_2)_2(SeO_3)_4(Se_2O_5)$, $Pb_2Nb_2Se_4O_{15}$, $PbMSeO_6$ (M = Mo and W), and $PbMo_2O_5(SeO_3)_2$.[7,8] Among them, six of them are structurally centrosymmetric and not SHG active; only $Pb_4(VO_2)_2(SeO_3)_4(Se_2O_5)$ is NCS and displays a moderately strong SHG response of approximately 150 × α-SiO_2.

In the transition metal selenite and tellurite halide systems, the halide anions can be regarded as "chemical scissors" since they prefer to coordinate with transition metals, whereas the Se^{4+} and Te^{4+} cations only bonded with oxygen atoms, which may lead to new low-dimensional magnetic materials.[9] Recently, our explorations of new SHG materials in the Pb^{2+}-(d^0-TM)-Se^{4+}-oxyhalide system resulted in two new polar materials, namely, $Pb_2TiOF(SeO_3)_2Cl$ and $Pb_2NbO_2(SeO_3)_2Cl$, which display an SHG response of approximately 9.6 × KDP and 2.3 × KDP, respectively.[10] Results of our studies indicate that whether F^- is involved in the d^0-TM coordination sphere or not considerably determines the differences in their band structures and thus the large differences in their SHG effects. As an extension of our previous work, this paper focuses on the Pb^{2+}-V^{5+}-Se^{4+}-oxyhalide system. The V^{5+} cation can adopt VO_4, VO_5, and VO_6 coordination geometries,[6e,f] and these polyhedra can be further interconnected into various anionic structures such as 1D chains, 2D sheets, or 3D networks in addition to isolated polynuclear clusters.[7a] Hence it is expected that the Pb^{2+}-V^{5+}-Se^{4+}-oxyhalide system will display much more rich structural chemistry than those containing Ti^{4+} and Nb^{5+} cations. Our research efforts in this aspect led to the isolation of three new mixed-metal selenites, namely,

Received: June 30, 2014
Published: August 7, 2014

   dx.doi.org/10.1021/ic501548m | Inorg. Chem. 2014, 53, 8816−8824

$Pb_4V_6O_{16}(SeO_3)_3(H_2O)$, $Pb_2VO_2(SeO_3)_2Cl$, and $PbVO_2(SeO_3)F$. Herein we report their syntheses, crystal structures, and optical properties.

EXPERIMENTAL SECTION

Materials and Instruments. $PbCl_2$ (99+%, AR), $PbCO_3$ (98+%, AR), V_2O_5 (99.5+%, AR), SeO_2 (99+%, AR), KOH (96+%, AR), and hydrofluoric acid (40+%, AR) were used as received. All of the chemicals were supplied by the Shanghai Reagent Factory. The 1 M KOH solution was obtained by dissolving 0.5611 g of KOH in 10 mL of H_2O.

Synthesis of $Pb_4V_6O_{16}(SeO_3)_3(H_2O)$. $Pb_4V_6O_{16}(SeO_3)_3(H_2O)$ was prepared by using hydrothermal techniques. A mixture of $PbCO_3$ (160.0 mg, 0.6 mmol), V_2O_5 (81.8 mg, 0.45 mmol), SeO_2 (166.4 mg, 1.5 mmol), 0.10 mL of a 1 M KOH solution, and H_2O (6 mL) was sealed in an autoclave equipped with a Teflon linear (23 mL) and heated at 230 °C for 4 days, followed by slow cooling to room temperature at a rate of 2 °C/h. The final pH value of the reaction media is close to 1.5. Yellow flake-shaped crystals of $Pb_4V_6O_{16}(SeO_3)_3(H_2O)$ were obtained as a single phase in a yield of about 73% based on Pb, and its purity was confirmed by X-ray diffraction (XRD) studies (Figure S1a). The result of EDS elemental analyses on several single crystals revealed an average molar ratio of Pb/V/Se of 1.25:2.12:1, which is very close to that determined from single-crystal X-ray structural studies.

Synthesis of $Pb_2VO_2(SeO_3)_2Cl$. $Pb_2VO_2(SeO_3)_2Cl$ was prepared by using hydrothermal techniques. The loaded compositions are $PbCl_2$ (111.2 mg, 0.4 mmol), V_2O_5 (45.5 mg, 0.25 mmol), SeO_2 (166.4 mg, 1.5 mmol), 0.10 mL of HF acid (~40%), and H_2O (6 mL), and the resultant mixture was heated at 220 °C for 4 days. The final pH value of the reaction media is close to 0.8. Garnet, brick-shaped single crystals of $Pb_2VO_2(SeO_3)_2Cl$ were obtained as a single phase in a yield of about 91% based on Pb, and its purity was confirmed by XRD studies (Figure S1b). Results of the energy dispersive spectrometry (EDS) elemental analyses on several single crystals revealed an average molar ratio of Pb/V/Se/Cl of 1.99:1:2.17:1.22, which is in good agreement with that determined from single-crystal X-ray structural studies.

$Pb_2VO_2(SeO_3)_2Cl$ can also be prepared by high-temperature solid-state reactions. A stoichiometric mixture of $PbCl_2$ (417.2 mg, 1.5 mmol), PbO (111.6 mg, 0.5 mmol), V_2O_5 (91.0 mg, 0.5 mmol), and SeO_2 (221.9 mg, 2 mmol) was thoroughly ground and pressed into a pellet. The pellet was sealed into a silica tube under vacuum. The tube was gradually heated to 450 °C, held for 20 h, and then cooled to room temperature. Defective crystals and excellent powders isolated were confirmed to be a single phase of $Pb_2VO_2(SeO_3)_2Cl$ by powder X-ray diffraction studies.

Synthesis of $PbVO_2(SeO_3)F$. A mixture of $PbCO_3$ (160.0 mg, 0.6 mmol), V_2O_5 (45.5 mg, 0.25 mmol), SeO_2 (166.4 mg, 1.5 mmol), and H_2O (6 mL) with a pH value preadjusted to 1.0 with the addition of a few drops of hydrofluoric acid (~40%) was sealed in an autoclave equipped with a Teflon liner (23 mL) and heated at 230 °C for 4 days. After washing with distilled water, large red, brick-like crystals of $PbVO_2(SeO_3)F$ were obtained in a yield of about 85% based on Pb, and its purity was confirmed by XRD powder diffraction study (Figure S1c). The EDS elemental analyses on several single crystals of $PbVO_2(SeO_3)F$ gave an average molar ratio of Pb/V/Se/F of 1.12:1:1.36:1.41, which is close to that determined from single-crystal X-ray structural studies.

Single-Crystal Structure Determination. A yellow, plate-shaped crystal of $Pb_4V_6O_{16}(SeO_3)_3(H_2O)$ (0.32 × 0.28 × 0.07 mm^3) and a garnet brick crystal of $Pb_2VO_2(SeO_3)_2Cl$ (0.23 × 0.21 × 0.08 mm^3) as well as a yellow brick crystal of $PbVO_2(SeO_3)F$ (0.51 × 0.36 × 0.19 mm^3) were used for single-crystal X-ray diffraction data collections. Data collections were performed on an Agilent Technologies SuperNova dual wavelength CCD diffractometer (for $Pb_4V_6O_{16}(SeO_3)_3(H_2O)$) with Cu K$\alpha$ radiation (λ = 1.54178 Å), a Saturn724 CCD diffractometer (for $Pb_2VO_2(SeO_3)_2Cl$), and a Mercury CCD diffractometer (for $PbVO_2(SeO_3)F$) with Mo Kα radiation (λ = 0.71073 Å) at 293 K. All three date sets were corrected for Lorentz and polarization factors as well as absorption by the multiscan method.[11a] All structures were solved by the direct methods and refined by full-matrix least-squares fitting on F^2 using SHELXL-97.[11b] All three structures were checked for possible missing symmetry elements with PLATON, and none was found.[11c] The Flack parameter was refined to 0.036(10) for $Pb_4V_6O_{16}(SeO_3)_3(H_2O)$, which confirms the correctness of its absolute structure. For $Pb_2VO_2(SeO_3)_2Cl$, two separate crystals were used for single-crystal X-ray data collections. The Flack parameters were refined to 0.347(12) and 0.40(4), respectively, indicative of the existence of the racemic twinning. Crystallographic data, structural refinements, and important bond distances are summarized in Tables 1 and 2, respectively. More crystallographic data on the compounds are given in the Supporting Information.

Table 1. Summary of Crystal Data and Structural Refinements for the Three Title Compounds

formula	$Pb_4V_6O_{16}(SeO_3)(H_2O)$	$Pb_2VO_2(SeO_3)_2Cl$	$PbVO_2(SeO_3)F$
fw	1789.30	786.69	436.09
cryst syst	monoclinic	monoclinic	orthorhombic
space group	$P2_1$	$P2_1$	*Pbca*
a/Å	7.13620(10)	8.333(3)	9.812(3)
b/Å	21.3103(4)	5.3171(16)	8.147(3)
c/Å	7.20040(10)	10.710(4)	13.026(4)
α/deg	90	90	90
β/deg	94.887(2)	111.701(5)	90
γ/deg	90	90	90
V/Å^3	1091.02(3)	440.9(2)	1041.3(6)
Z	2	2	8
D_c/g·cm^{-3}	5.447	5.926	5.563
μ(Mo K*a*)/mm^{-1}	86.086	47.700	41.045
GOF on F^2	1.042	0.920	1.040
Flack factor	0.036(10)	0.347(12)	
R1, wR2 $[I > 2\sigma(I)]^a$	0.0317, 0.0785	0.0233, 0.0431	0.0308, 0.0718
R1, wR2 (all data)	0.0323, 0.0788	0.0248, 0.0434	0.0339, 0.0734

^{a}R1 = $\sum||F_o| - |F_c||/\sum|F_{ol}$, wR2 = $\{\sum w[(F_o)^2 - (F_c)^2]^2/\sum w[(F_o)^2]^2\}^{1/2}$.

Powder XRD. The X-ray powder diffraction patterns for the three compounds were collected in continuous mode on a Rigaku MiniFlex II diffractometer at room temperature (Cu Kα radiation). Data were collected in the 2θ range of 5−70° with a step size of 0.02°.

Energy Dispersive Spectrometry. Elemental analyses were carried out on a field emission scanning electron microscope (JSM6700F) equipped with an energy dispersive X-ray spectroscope (Oxford Inc.).

IR Spectroscopy. Infrared spectra were collected on a Magna 750 FT-IR spectrometer as KBr pellets in the range of 4000−400 cm^{-1} with a resolution of 2 cm^{-1} at room temperature.

UV−Vis and IR Transmission Spectra. The UV−vis diffuse reflectance spectra were measured with a PE Lambda 900 UV−vis−NIR spectrophotometer at 190−2500 nm at room temperature. A $BaSO_4$ plate was used as a standard (100% reflectance) for the baseline correction. The absorption spectrum was converted from reflectance spectra using the Kubelka−Munk function: $\alpha/S = (1 - R)^2/2R = K/S$,[12] where α, R, S, and K represent the absorption coefficient, reflectance, scattering coefficient, and absorption, respectively.

Thermal Analysis. Thermogravimetric analysis (TGA) and differential scanning calorimetry were performed with a Netzch STA449C unit at a heating rate of 10 °C/min under a N_2 atmosphere.

SHG Measurements. SHG measurements for $Pb_4V_6O_{16}(SeO_3)_3(H_2O)$ and $Pb_2VO_2(SeO_3)_2Cl$ were performed at

dx.doi.org/10.1021/ic501548m | Inorg. Chem. 2014, 53, 8816−8824

Table 2. Selected Bond Distances (Å) for the Three Title Compounds

$Pb_4V_6O_{16}(SeO_3)_3(H_2O)$					
Pb(1)−O(8)	2.359(14)	Pb(4)−O(10)	2.475(9)	V(4)−O(10)	1.668(8)
Pb(1)−O(3)	2.462(11)	Pb(4)−O(13)	2.527(10)	V(4)−O(4)	1.919(9)
Pb(1)−O(16)	2.525(10)	Pb(4)−O(6)	2.558(10)	V(4)−O(9)	1.920(11)
Pb(1)−O(18)	2.577(10)	Pb(4)−O(24)	2.611(11)	V(4)−O(15)	2.020(10)
Pb(1)−O(25)	2.580(10)	Pb(4)-O(1W)	2.64(2)	V(5)−O(23)	1.622(9)
Pb(1)−O(14)	2.607(10)	Pb(4)−O(20)	2.678(10)	V(5)−O(19)	1.740(10)
Pb(1)−O(5)	2.714(11)	Pb(4)−O(22)	2.788(10)	V(5)−O(21)	1.851(9)
Pb(2)−O(6)	2.486(10)	Pb(4)−O(2)	2.845(10)	V(5)−O(11)	1.900(10)
Pb(2)−O(19)	2.551(9)	V(1)−O(24)	1.621(12)	V(5)−O(17)	1.981(10)
Pb(2)−O(14)	2.634(10)	V(1)−O(13)	1.682(10)	V(6)−O(22)	1.614(10)
Pb(2)−O(1)	2.749(9)	V(1)−O(17)	1.907(9)	V(6)−O(15)	1.733(11)
Pb(2)−O(20)	2.750(10)	V(1)−O(12)	1.908(9)	V(6)−O(12)	1.861(10)
Pb(2)−O(2)	2.757(10)	V(1)−O(11)	1.974(10)	V(6)−O(17)	1.893(9)
Pb(2)−O(5)	2.793(11)	V(2)−O(25)	1.601(10)	V(6)−O(21)	2.069(10)
Pb(2)−O(23)	2.879(10)	V(2)−O(14)	1.680(10)	Se(1)−O(2)	1.695(9)
Pb(2)−O(16)	2.937(11)	V(2)−O(11)	1.886(10)	Se(1)−O(3)	1.706(10)
Pb(3)−O(3)	2.519(10)	V(2)−O(21)	1.906(10)	Se(1)−O(1)	1.752(9)
Pb(3)−O(15)	2.549(10)	V(2)−O(12)	2.092(10)	Se(2)−O(6)	1.690(10)
Pb(3)−O(18)	2.674(10)	V(3)−O(18)	1.632(10)	Se(2)−O(5)	1.691(10)
Pb(3)−O(10)	2.686(9)	V(3)−O(16)	1.641(10)	Se(2)−O(4)	1.744(9)
Pb(3)−O(13)	2.716(10)	V(3)−O(19)	1.955(10)	Se(3)−O(7)	1.712(11)
Pb(3)−O(4)	2.737(9)	V(3)−O(1)	1.962(9)	Se(3)−O(8)	1.721(14)
Pb(3)−O(2)	2.801(10)	V(3)−O(7)	1.978(12)	Se(3)−O(9)	1.725(10)
Pb(3)−O(5)	2.837(10)	V(4)−O(20)	1.638(10)		
		$Pb_2VO_2(SeO_3)_2Cl$			
Pb(1)−O(3)	2.569(7)	Pb(2)−O(4)	2.565(8)	V(1)−O(6)	2.108(7)
Pb(1)−O(6)	2.571(7)	Pb(2)−O(5)	2.703(9)	V(1)−O(2)	2.124(8)
Pb(1)−O(5)	2.588(9)	Pb(2)−O(5)	2.798(9)	Se(1)−O(3)	1.674(7)
Pb(1)−O(4)	2.700(9)	Pb(2)−Cl(1)	2.912(3)	Se(1)−O(2)	1.701(8)
Pb(1)−O(2)	2.777(8)	Pb(2)−O(8)	2.971(6)	Se(1)−O(1)	1.742(8)
Pb(1)−O(1)	2.983(8)	Pb(2)−Cl(1)	3.044(3)	Se(2)−O(5)	1.694(8)
Pb(1)−O(1)	3.010(8)	V(1)−O(8)	1.627(6)	Se(2)−O(6)	1.702(7)
Pb(1)−Cl(1)	3.047(3)	V(1)−O(7)	1.702(7)	Se(2)−O(4)	1.726(9)
Pb(2)−O(4)	2.487(9)	V(1)−O(1)	1.990(8)		
Pb(2)−O(3)	2.540(7)	V(1)−O(7)	1.993(7)		
		$PbVO_2(SeO_3)F$			
Pb(1)−O(1)	2.500(6)	Pb(1)−O(5)	2.748(5)	V(1)−O(4)	1.685(5)
Pb(1)−F(1)	2.525(5)	Pb(1)−O(3)	2.799(6)	V(1)−O(3)	1.966(5)
Pb(1)−F(1)	2.569(5)	Se(1)−O(1)	1.672(6)	V(1)−O(2)	1.993(5)
Pb(1)−O(2)	2.576(5)	Se(1)−O(3)	1.735(5)	V(1)−F(1)	2.003(5)
Pb(1)−O(4)	2.583(5)	Se(1)−O(2)	1.741(5)	V(1)−O(4)	2.294(5)
Pb(1)−O(1)	2.671(5)	V(1)−O(5)	1.627(6)		

room temperature on sieved powder samples (100−210 μm) using a pulsed Nd:YAG laser with a wavelength of 532 nm, 1064 nm, 1400 nm, and 2.05 μm, respectively.[13] In order to evaluate relative SHG efficiencies of the compound, a KDP sample with the same particle size was used as the reference.

Polarization Properties. The polarization properties of $Pb_4V_6O_{16}(SeO_3)_3(H_2O)$ and $Pb_2VO_2(SeO_3)_2Cl$ were measured on an aixACCT TF Analyzer 2000E ferroelectric tester at room temperature. The powder was pressed into a pellet (5 mm diameter and 0.4 mm thick), and the conducting Ag glue was applied on the both sides of the pellet surfaces for electrodes.

Computational Descriptions. Single-crystal structural data of the three compounds were used for the theoretical calculations. The electronic structure calculations including band structures and density of states (DOS) were performed with the total-energy code CASTEP.[14] The total energy was calculated with density functional theory (DFT) using Perdew−Burke−Ernzerhof generalized gradient approximation.[15] The interactions between the ionic cores and the electrons were described by the norm-conserving pseudopotential.[16] The following orbital electrons were treated as valence electrons: Pb-$5d^{10}6s^26p^2$, V-$3d^34s^2$, Se-$4s^24p^4$, O-$2s^22p^4$, F-$2s^22p^5$, Cl-$3s^23p^5$, and H-$1s^1$. The numbers of plane waves included in the basis sets were determined by a cutoff energy of 820, 820, and 850 eV for $Pb_4V_6O_{16}(SeO_3)_3(H_2O)$, $Pb_2VO_2(SeO_3)_2Cl$, and $PbVO_2(SeO_3)F$, respectively. The numerical integration of the Brillouin zone was performed using a Monkhorst-Pack k-point sampling of 4 × 1 × 3, 3 × 5 × 3, and 3 × 3 × 2, respectively. The other parameters and convergent criteria were the default values of the CASTEP code.

RESULTS AND DISCUSSION

Syntheses. Three new lead(II)−vanadium(V) mixed-metal selenites, namely, $Pb_4V_6O_{16}(SeO_3)_3(H_2O)$, $Pb_2VO_2(SeO_3)_2Cl$, and $PbVO_2(SeO_3)F$, have been successfully synthesized by hydrothermal reactions under different reaction conditions. Their syntheses use V_2O_5 and SeO_2 for the V and Se sources, $PbCl_2$ or $PbCO_3$ as the lead(II) source, and KOH or HF as the pH mediator and mineralizer. During the preparations of

dx.doi.org/10.1021/ic501548m | Inorg. Chem. 2014, 53, 8816−8824

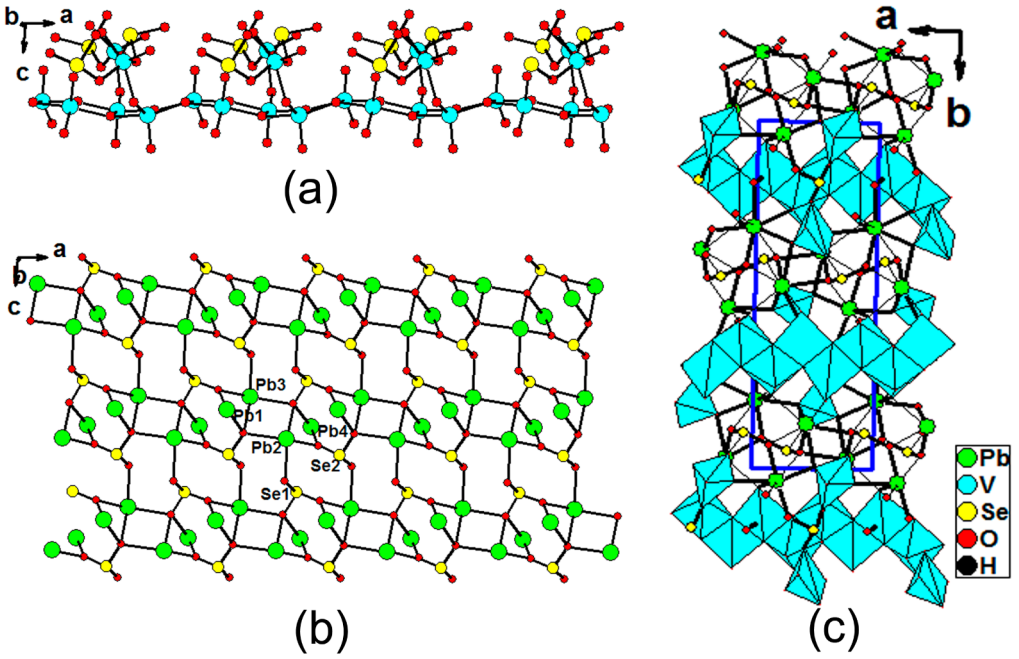

Figure 1. 1D $[V_6O_{16}(SeO_3)_3]^{8-}$ chain along the *a* axis (a), 2D $[Pb_4(SeO_3)_2]^{4+}$ layer parallel to the *ac* plane (b), view of the structure of $Pb_4V_6O_{16}(SeO_3)_3(H_2O)$ along the *c* axis (c). Pb, V, Se, O, and H atoms are drawn as green, cyan, yellow, red, and black circles, respectively, and VO_5 polyhedra are shaded in cyan.

$PbVO_2(SeO_3)F$, HF also acts as the source of the F^- anion. All three compounds were synthesized under acidic conditions. It is found that HF played an important role. Under the presence of HF, $Pb_2VO_2(SeO_3)_2Cl$ and $PbVO_2(SeO_3)F$ were obtained by using $PbCl_2$ and $PbCO_3$ as the lead sources. $Pb_2VO_2(SeO_3)_2Cl$ can also be prepared by standard high-temperature solid-state reactions. However, the hydrothermal method with the addition of HF as mineralizer yielded single crystals with much better quality.

Structure of $Pb_4V_6O_{16}(SeO_3)_3(H_2O)$. $Pb_4V_6O_{16}(SeO_3)_3(H_2O)$ crystallizes in the noncentrosymmetric and polar space group $P2_1$ (No. 4). The structure of $Pb_4V_6O_{16}(SeO_3)_3(H_2O)$ can be described as 2D lead(II) selenite layers parallel to the *ac* plane being bridged by 1D $[V_6O_{16}(SeO_3)_3]^{8-}$ chains, which propagate along the *a* axis (Figure 1). Its asymmetric unit contains four Pb^{2+}, six V^{5+}, and three Se^{4+} cations. All three Se^{4+} cations are in the asymmetric coordination environments attributed to SOJT effects; they are in ψ-SeO_3 trigonal pyramidal geometry with the pyramidal site occupied by the lone pair electrons. The Se−O bond lengths range from 1.690(10) to 1.752(9) Å (Table 2). All six V^{5+} cations are in distorted trigonal bypyramidal geometries composed of five oxygen atoms.[7a,17] V(1), V(2), V(5), and V(6) are coordinated by five oxo anions, whereas V(3) and V(4) are coordinated by three oxo anions and two unidentate selenite anions. The five V−O bonds are two short (1.614(12)−1.733(11) Å) and three normal (1.866(10)−2.069(10) Å) (Table 2). $V(1)O_5$, $V(2)O_5$, $V(5)O_5$, and $V(6)O_5$ are interconnected via edge- and corner-sharing into a 1D $[V_4O_{12}]^{4-}$ ladder chain (Figure S2a). $V(3)O_5$ and $V(4)O_5$ units are bridged by a $Se(3)O_3$ group into a dinuclear $[V_2O_6(SeO_3)_3]^{8-}$ unit (Figure S2b). The $[V_2O_6(SeO_3)_3]^{8-}$ units are grafted into the $[V_4O_{12}]^{4-}$ chain via V−O−V bridges to form a $[V_6O_{16}(SeO_3)_3]^{8-}$ branched chain (Figure 1a).

It is interesting to compare the structure of $[V_6O_{16}(SeO_3)_3]^{8-}$ with those of other vanadium oxide substructures reported in $Th(VO_3)_2(SeO_3)$ and $La(VO_3)_2(IO_3)$,[17] whose structures exhibit similar $(V_2O_6)^{2-}$ ladder chains as in $Pb_4V_6O_{16}(SeO_3)_3(H_2O)$; however, the selenite or idodate groups in $Th(VO_3)_2(SeO_3)$ and $La(VO_3)_2(IO_3)$ are not involved in the coordination with vanadium(V) cations. Furthermore, no additional vanadium atoms are available to function as branches to the chains.

The four unique lead(II) atoms in $Pb_4V_6O_{16}(SeO_3)_3(H_2O)$ exhibit different coordination environments. The Pb(1) atom is seven coordinated by three unidentate SeO_3 groups and four oxo anions, the Pb(2) atom is nine-coordinated by four unidentate SeO_3 groups and five oxo anions, the Pb(3) atom is eight-coordinated by four unidentate SeO_3 groups as well as four oxo anions, whereas the Pb(4) atom is eight-coordinated by two unidentate SeO_3 groups, five oxo anions, and an aqua ligand (Figure S3a−d). The Pb−O bond lengths are in the ranges of 2.359(14)−2.937(11) Å. Bond valence calculations on $Pb_4V_6O_{16}(SeO_3)_3(H_2O)$ gave values of 1.75−2.22, 3.84−3.97, 5.00−5.16, and −1.76 to −2.42 for Pb, Se, V, and O atoms, respectively, indicating they are in oxidation state 2+, 4+, 5+, and 2−, respectively.[18]

It is interesting to note that the interconnection of Pb^{2+} ions by bridging $Se(1)O_3$ and $Se(2)O_3$ groups forms a 2D lead(II) selenite layer parallel to the *ac* plane (Figure 1b). The above vanadium selenite chains and lead selenite layers are interconnected by Pb−O−V and Pb−O−Se bridges into a complicated 3D network (Figure 1c). The three selenite groups display two different coordination modes (Figure S2c−e). $Se(1)O_3$ and $Se(2)O_3$ groups connect with one V^{5+} and six Pb^{2+} cations each, whereas the $Se(3)O_3$ group connects with only one Pb^{2+} and two V^{5+} cations.

Structure of $Pb_2VO_2(SeO_3)_2Cl$. $Pb_2VO_2(SeO_3)_2Cl$ crystallizes in the noncentrosymmetric and polar space group $P2_1$ (No. 4), and it is isostructural with $Pb_2TiOF(SeO_3)_2Cl$ and $Pb_2NbO_2(SeO_3)_2Cl$.[10] $Pb_2VO_2(SeO_3)_2Cl$ exhibits a complicated 3D network composed of novel 1D $[VO_2(SeO_3)_2]^{3-}$

dx.doi.org/10.1021/ic501548m | Inorg. Chem. 2014, 53, 8816−8824

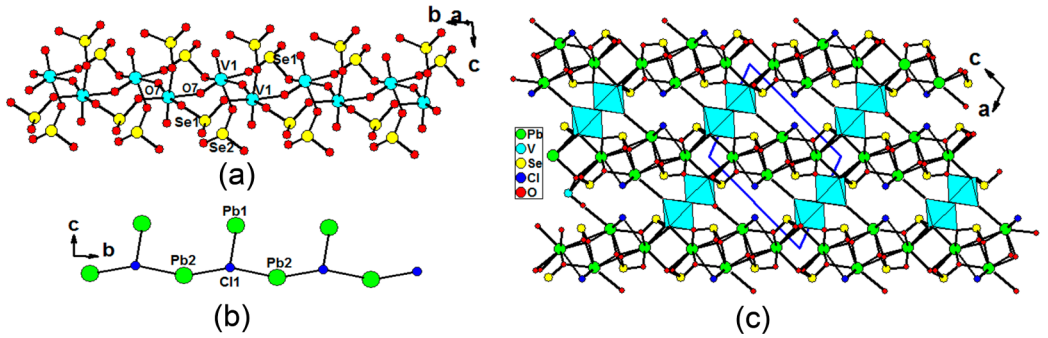

Figure 2. 1D $[VO_2(SeO_3)_2]^{3-}$ anionic chain along the *b* axis (a), 1D $[Pb_2Cl]^{3+}$ cationic chain along the *b* axis (b), and view of the structure of $Pb_2VO_2(SeO_3)_2Cl$ down the *b* axis (c). Pb, V, Se, O, and Cl atoms are drawn as green, cyan, yellow, red, and blue circles, respectively. VO_6 octahedra are shaded in cyan.

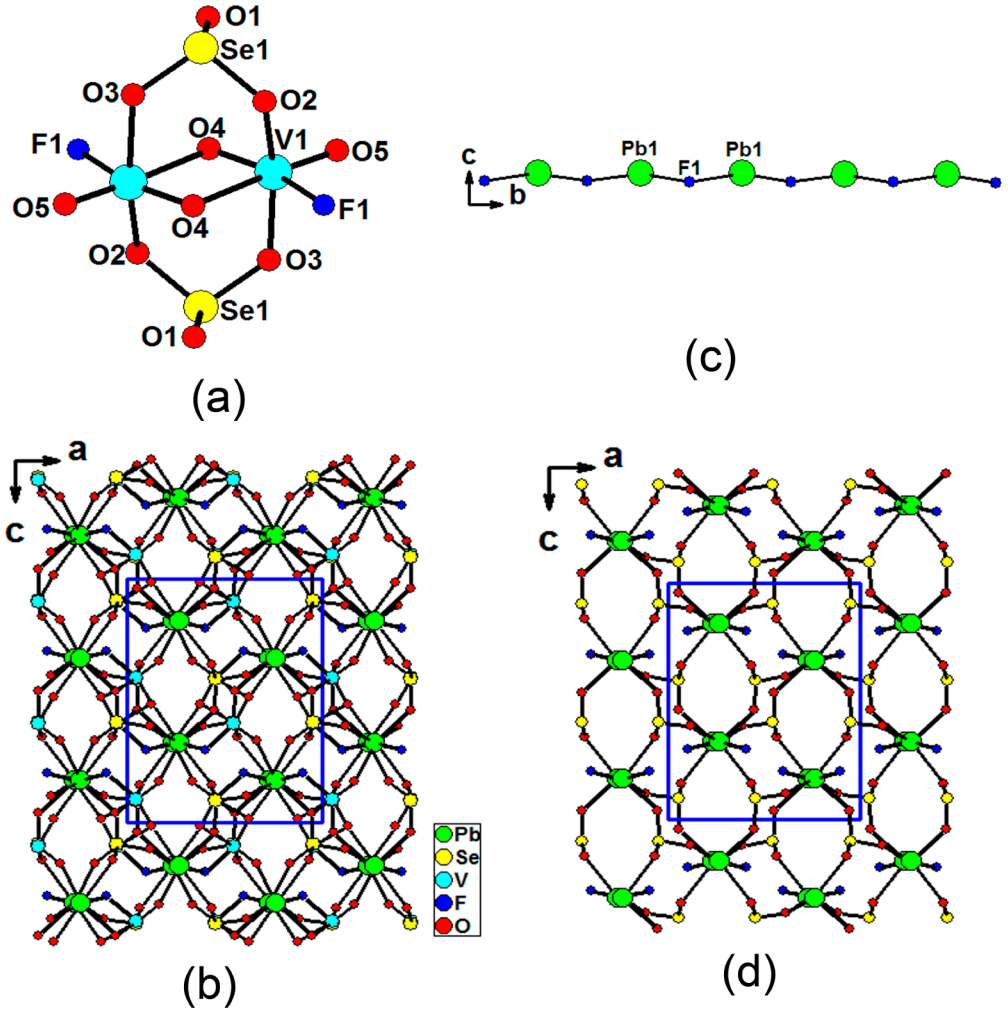

Figure 3. $[V_2O_4(SeO_3)_2F_2]^{4-}$ unit (a), view of the structure of $PbVO_2(SeO_3)F$ down the *b* axis (b), 1D $[PbF]^+$ cationic chain along the *b* axis (c), and view of the 3D network of lead(II) selenite fluoride down the *b* axis in $PbVO_2(SeO_3)F$ (d). Pb, V, Se, O, and F atoms are drawn as green, cyan, yellow, red, and blue circles, respectively.

anionic chains that are interconnected by 1D $[Pb_2Cl]^{3+}$ cationic chains (Figure 2). The $[VO_2(SeO_3)_2]^{3-}$ anionic chain along the *b* axis consists of a 1D chain of corner-sharing VO_6 octahedra, which is further decorated by selenite groups in a bidentate bridging or unidentate fashion (Figure 2a). The asymmetric unit of $Pb_2VO_2(SeO_3)_2Cl$ contains two Pb^{2+}, one Ti^{4+}, two Se^{4+}, and one Cl^- atom. Both the V^{5+} and Se^{4+} cations are in the asymmetric coordination environments attributed to SOJT effects. The V^{5+} cation is in a distorted octahedral geometry composed of three selenite oxygen atoms from three selenite groups and three oxo anions. The V−O bond distances are two long [2.105(7)−2.123(9) Å], two short [1.628(6) Å−1.703(7) Å], and two normal [1.988(8)−1.993(7) Å]; hence the VO_6 octahedron is distorted toward an edge (local C_2 direction). The magnitude of the out-of-center distortion (Δd) was calculated to be 0.8708,[4] which is close to those for the NbO_6

dx.doi.org/10.1021/ic501548m | *Inorg. Chem.* 2014, 53, 8816−8824

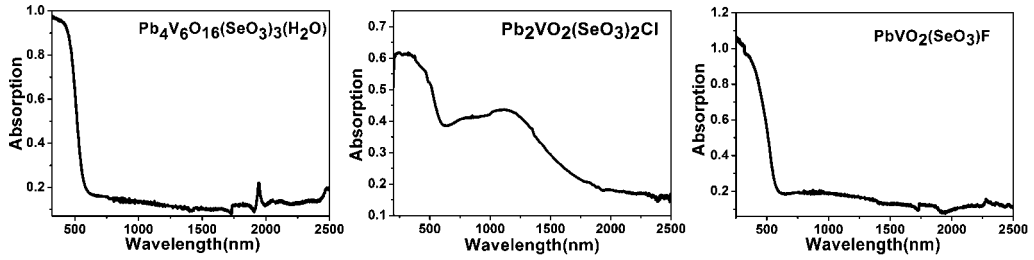

(a) (b) (c)

Figure 4. UV−vis absorption spectra of $Pb_4V_6O_{16}(SeO_3)_3(H_2O)$ (a), $Pb_2VO_2(SeO_3)_2Cl$ (b), and $PbVO_2(SeO_3)F$ (c).

in $Pb_2NbO_2(SeO_3)_2Cl$, but is slightly larger than that for TiO_5F in $Pb_2TiOF(SeO_3)_2Cl$.[10] The two unique Se^{4+} cations are in a ψ-SeO_3 trigonal pyramidal environment with the pyramidal site occupied by the lone-pair electrons. The Se−O bond lengths range from 1.675(7) to 1.743(8) Å. Neighboring VO_6 octahedra are interconnected via corner-sharing (O7) into a zigzag 1D chain along the *b* axis. Each $Se(1)O_3$ group bridges with two interval V^{5+} cations and forms a V_3Se four-membered ring, whereas $Se(2)O_3$ groups are attached on the chain unidentately (Figure 2a).

The Pb(1) atom is eight coordinated by two bidentate chelating and three unidentate SeO_3 groups as well as a chloride anion, whereas the Pb(2) atom is eight-coordinated by one bidentate chelating and three unidentate SeO_3 groups, two chloride anions, and an oxo anion (Figure S4). The Pb−O and Pb−Cl bond lengths are in the ranges 2.539(7)−2.984(9) and 3.011(9)−3.047(3) Å, respectively. Bond valence calculations on $Pb_2VO_2(SeO_3)_2Cl$ gave values of 1.66−2.03, 3.97−3.98, 4.98, −0.86, and −1.7 to −2.11 for Pb, Se, V, Cl, and O atoms, respectively, indicating they are in oxidation states of 2+, 5+, 4+, 1−, and 2−, respectively.[18]

It is interesting to note that the interconnection of lead(II) ions by chloride anions resulted in a cationic chain of $(Pb_2Cl)^{3+}$ also along the *b* axis (Figure 2b). The above cationic and anionic 1D chains are further interconnected by Pb−O bonds into a complicated 3D framework (Figure 2c). Alternatively, the 3D network of $Pb_2VO_2(SeO_3)_2Cl$ can also be viewed as a pillared layered structure composed of (−1 0 1) lead(II) selenium(IV) oxychloride layers that are cross-linked by the vanadium oxide chains. One lead(II)−selenium(IV) oxychloride layer is shown in Figure S5a. The two unique selenite groups adopt different coordination modes (Figure S5b). $Se(1)O_3$ is hexadentate and bridges with two V and four Pb atoms, whereas $Se(2)O_3$ is octadentate; it forms a bidentate chelation with Pb(1) (O4, O6) and another bidentate chelation with Pb(2) (O4, O5) and also bridges with a V atom and three additional Pb atoms.

Structure of $PbVO_2(SeO_3)F$. $PbVO_2(SeO_3)F$ crystallizes in the centrosymmetric space group *Pbca* (No. 61). The structure of $PbVO_2(SeO_3)F$ features $[V_2O_4(SeO_3)_2F_2]^{4-}$ dimers that are further bridged by Pb^{2+} cations in a 3D network (Figure 3b). There are one Pb^{2+} cation, one V^{5+} cation, one fluoride, and two unique selenite anions in the asymmetric unit of $PbVO_2(SeO_3)F$. The V^{5+} cation is six-coordinated by two selenite groups in a unidentate fashion and one F^- and three O^{2-} anions in a severely distorted octahedral geometry. Two VO_5F octahedra form a dimer via edge-sharing (O4···O4), and the two SeO_3 groups are attached to both sides of the dimer in a bidentate bridging mode (Figure 3a). The V−O(F) bond distances are two short [1.627(6)−1.685(5) Å], two normal [1.966(5)−1.993(5) Å], and two long [2.003(5) (V−F)−2.294(5) Å]; hence the VO_5F octahedron is distorted toward an edge (local C_2 direction). The magnitude of the out-of-center distortion (Δd) was calculated to be 1.0414,[4] which is comparable to those in $Pb_2V_3Se_5O_{18}$.[8a] The Se(1) atom is three-coordinated by three O atoms in a distorted ψ-SeO_3 tetrahedral geometry, with the fourth site occupied by the lone-pair electrons, which is very common in metal selenites. The Se−O distances fall in the range 1.672(6)−1.741(5) Å.

The Pb^{2+} ion is eight-coordinated by four selenite groups in a unidentate fashion and three oxo as well as two fluoride anions (Figure S6a). The Pb−O and Pb−F distances are in the range 2.500(6)−2.799(6) and 2.525(5)−2.569(5) Å, respectively. Bond valence sum calculations gave total bond valences of 1.97, 4.95, 3.89, and −0.94 for Pb(1), V(1), Se(1), and F(1) atoms, respectively, indicating the oxidation states of Pb, Se, V, and F atoms are 2+, 4+, 5+, and 1−, respectively.[18] Each selenite anion is hexadentate and bridges with two vanadium(V) and four lead(II) atoms (Figure S6b).

It is interesting to note that the interconnection of lead(II) ions by selenite and fluoride anions forms a complicated 3D network (Figure 3d). Such a network can be viewed as 1D PbF chains along the *b* axis (Figure 3c) being further bridged by selenite groups.

TGA. Results of the TGA and DTA analyses indicate that $Pb_4V_6O_{16}(SeO_3)_3(H_2O)$, $Pb_2VO_2(SeO_3)_2Cl$, and $PbVO_2(SeO_3)F$ are stable up to 310, 322, and 265 °C, respectively (Figure S7). $Pb_4V_6O_{16}(SeO_3)_3(H_2O)$ reveals one step of weight loss in the temperature range 322−412 °C. The weight loss of 19.8% corresponds to the release of 1 mol of H_2O and 3 mol of SeO_2 per formular unit (calculated value: 19.6%).

$Pb_2VO_2(SeO_3)_2Cl$ displays two main steps of weight loss in the temperature range 310−696 °C and exhibits two endothermic peaks at 391 and 537 °C, during which 2 mol of SeO_2 and 0.5 mol of Cl_2 per formular unit are released.

$PbVO_2(SeO_3)F$ also exhibits one main step of weight loss in the temperature range 265−680 °C, which corresponds to the release of 1 mol of SeO_2 and 0.5 mol of F_2 per formula unit. The observed weight loss of 29.4% for $PbVO_2(SeO_3)F$ is close to the calculated one (29.8%). The final residuals were not characterized due to their melting with the TGA buckets (made of Al_2O_3) under high temperatures.

Optical Properties. The IR spectra of $Pb_4V_6O_{16}(SeO_3)_3(H_2O)$, $Pb_2VO_2(SeO_3)_2Cl$, and $PbVO_2(SeO_3)F$ have been measured in the wavenumber range 4000−400 cm^{-1} at room temperature (Figure S8, Table S1). $Pb_2VO_2(SeO_3)_2Cl$ and $PbVO_2(SeO_3)F$ are transparent in the range 4000−1000 cm^{-1}, whereas $Pb_4V_6O_{16}(SeO_3)_3(H_2O)$ shows a few absorption bands around

dx.doi.org/10.1021/ic501548m | *Inorg. Chem.* 2014, 53, 8816−8824

3530 and 1626 cm^{-1} attributable to O−H and H−O−H vibrations.[20] The bands associated with the Se−O, V−O(F), and O(F)−V−O(F) vibrations appeared at 400−1000 cm^{-1}. The absorption bands around 950−850, 850−600, and 550−400 cm^{-1} can be assigned to ν(Se−O), ν(V−O/F), and ν(O/F−V−O/F), respectively.[7a,8a]

UV−vis absorption spectra of each compound show one strong absorption peak at 630 nm (Figure 4), which originates from the charge transfer transition from O to V.[21] For compound **1**, the sharp absorption peak around 1946 nm is due to the water molecule in the structure. The broad absorption peak centered at 1127 nm for **2** can be assigned to charge transfer associated with V^{5+}.[22−24] Optical diffuse reflectance spectrum measurements reveal band gaps of about 2.54, 2.41, and 2.69 eV for $Pb_4V_6O_{16}(SeO_3)_3(H_2O)$, $Pb_2VO_2(SeO_3)_2Cl$, and $PbVO_2(SeO_3)F$ (Figure S9), respectively; hence all three compounds are wide band gap semiconductors.

Second-Harmonic Generation Properties. It is worth examining the SHG properties of $Pb_4V_6O_{16}(SeO_3)_3(H_2O)$ and $Pb_2VO_2(SeO_3)_2Cl$ due to their polar structures. For $Pb_2VO_2(SeO_3)_2Cl$, no SHG signal was detected under a Q-switched Nd:YAG laser at several typical wavelengths, which is probably due to the dark color of the material and the racemic twinning problem. $Pb_4V_6O_{16}(SeO_3)_3(H_2O)$ displays a weak SHG response of approximately 0.2 × KDP in the particle size range 100−210 μm under 1400 nm laser radiation (Figure 5).

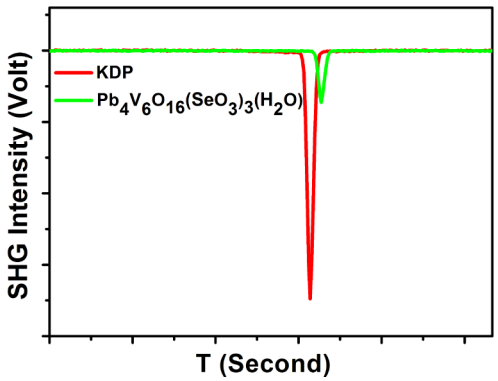

Figure 5. Oscilloscope traces of the SHG signals for the powders (100−210 μm) of KDP and $Pb_4V_6O_{16}(SeO_3)_3(H_2O)$ on a 1400 nm Q-switched laser. The curve drawn is to guide the eye and not a fit to the data.

To better understand the magnitude and direction of the dipole moments, the local dipole moments for the SeO_3, VO_5, and VO_6 groups and Pb coordination polyherda and the net dipole moments within a unit cell for $Pb_4V_6O_{16}(SeO_3)_3(H_2O)$ and $Pb_2VO_2(SeO_3)_2Cl$ were calculated by using a method reported earlier.[25] For $Pb_4V_6O_{16}(SeO_3)_3(H_2O)$, the calculated dipole moments for the PbO_x (x = 7, 8, 9), VO_5, and SeO_3 polyhedra are 2.65−4.39, 3.68−7.12, and 7.71−9.71 D, respectively (Table S2), which is consistent with the previously reported values.[26] The x, y, and z components of the polarizations from two $Pb(1)O_7$ polyhedra in a unit cell are 2 × (±1.32 D), 2 × (−0.92 D), and 2 × (±4.09 D), respectively. Hence, the x and z components of the polarizations from two $Pb(1)O_7$ polyhedra canceled out completely, and only the y component of their polarizations constructively adds to a small value of −1.84 D. As for the two $Pb(2)O_9$ polyhedra in a unit cell, the x, y, and z components of their polarizations are 2 × (±0.95 D), 2 × 0.94 D, and 2 × (±2.29 D), respectively. Thus, the x and z components of their polarizations cancel out completely, whereas those of the y component constructively add to a value of 1.88 D. Similarly, the x and z components of the polarizations associated with two $Pb(3)O_8$, two $Pb(4)O_8$, two $Se(1)O_3$, two $Se(2)O_3$, two $Se(3)O_3$, and all VO_5 polyhedra in a unit cell cancel out. Along the b axis, the y component of all PbO_x, SeO_3, and VO_5 polyhedra produce a net dipole moment of 8.36, −6.7, and −2.38 D, respectively (minus means they hold the opposite direction). A small net moment of 0.72 D along the $-b$ axis is obtained, which is consistent with the weak SHG signal observed. For $Pb_2VO_2(SeO_3)_2Cl$, the calculated dipole moments for the PbO_xCl_y, VO_6, and SeO_3 polyhedra are 6.58−8.95, 7.21, and 9.25−9.66 D. The x and z components of the polarizations from $Pb(1)O_7Cl$, $Pb(2)O_6Cl$, $Se(1)O_3$, $Se(2)O_3$, and $V(1)O_6$ polyhedra canceled out completely, whereas those of the y component add to a small net value of 2.30 D. Hence, for both $Pb_4V_6O_{16}(SeO_3)_3(H_2O)$ and $Pb_2VO_2(SeO_3)_2Cl$, the polarizations from different asymmetric groups have been largely canceled out.

Polarization Properties. Compounds **1** and **2** are polar; hence it is worthy to study their ferroelectric behavior. Ferroelectric measurements on pellets for $Pb_4V_6O_{16}(SeO_3)_3(H_2O)$ and $Pb_2VO_2(SeO_3)_2Cl$ (5 mm diameter and 0.4 mm thick) showed "polarization loops", which are frequency dependent (Figure S10) and revealed small remanent polarizations of 0.21 and 0.29 $\mu C/cm^2$ for $Pb_4V_6O_{16}(SeO_3)_3(H_2O)$ and $Pb_2VO_2(SeO_3)_2Cl$, respectively; hence their ferroelectric properties are negligible. These loops are likely attributable to dielectric loss, and the macroscopic polarization cannot be reversed in the presence of an external electric field. As is known, for ferroelectric materials, macroscopic polarization must be switchable or reversible in the presence of an external electric field, which requires that the local moments can also be reversed. For $Pb_4V_6O_{16}(SeO_3)_3(H_2O)$ and $Pb_2VO_2(SeO_3)_2Cl$, the local dipole moments of SeO_3, VO_6 (VO_5), and Pb coordination polyhedra must be reversed for ferroelectric behavior to occur. It is unlikely that the dipole moments associated with the asymmetric SeO_3 polyhedra can be reversible as reported by other groups.[1,3a,26] Thus, both materials are not ferroelectric. This is also in good agreement with the very small net dipole moments for both compounds.

Theoretical Calculations. To gain further insights on the electronic properties of the three compounds, theoretical calculations based on DFT methods were performed.

The results of band structure analysis are presented in Figure S11. The state energies of the lowest conduction band (L-CB) and the highest valence band (H-VB) of the compounds are presented in Table S3. For $Pb_4V_6O_{16}(SeO_3)_3(H_2O)$, the L-CB (2.23 eV) and H-VB (0.0 eV) are located at the Y point and G point, respectively, which reveals an indirect band gap of 2.23 eV. $Pb_2VO_2(SeO_3)_2Cl$ and $PbVO_2(SeO_3)F$ also display an indirect band gap of 2.41 and 2.85 eV, respectovely. These values are close to the experimental values (2.54, 2.11, and 2.69 eV, respectively). The bands can be assigned according to the total and partial DOS, as plotted in Figure S12. For $Pb_4V_6O_{16}(SeO_3)_3(H_2O)$, the bottom-most VBs ranging from −21.1 to −19.2 eV are constituted of Se-4s, H-1s, O-2s, and small amounts of Se-4p states. The VBs between −18.2 and −14.3 eV originate from O-2s, Pb-5d, and small amounts of Se-4p, whereas the VBs between −10.6 and −8.7 eV are mainly Se-

dx.doi.org/10.1021/ic501548m | Inorg. Chem. 2014, 53, 8816−8824

4s, H-1s states mixing with small amounts of O-2p states. In addition, in the range −7.6 to −6.2 eV, the VBs are composed of Pb-6s overlapping fully with small amounts of O-2p and Se-4p states. It is obvious that O-2p states are dominant around the Fermi level (−6.5 to 6.5 eV). In the regions of −6.5 to 0 eV and 1.7 to 8.6 eV, O-2p states overlap fully with Se-4p, V-3d, and Pb-6p, mixing with a small amount of Se-4s state, which indicates the clearly defined V−O coordination in distorted polyhedra and Se−O covalent interactions. The DOS curves of $Pb_2VO_2(SeO_3)_2Cl$ and $PbVO_2(SeO_3)F$ are very similar to those of $Pb_4V_6O_{16}(SeO_3)_3(H_2O)$ except for the involvement of halogen (F or Cl).

Population analyses provide more quantitative information. The calculated bond orders for Pb−O/F/Cl, V−O/F, and Se−O bonds are 0.01−0.22, 0.15−0.92, and 0.25−0.72 e, respectively, for the three compounds, which indicate that the Pb−O(F, Cl) bonds have more ionic character, whereas the V−O/F and Se−O bonds are much more covalent. In addition, to further verify whether the lone-pair electrons on the Pb^{2+} and Se^{4+} cations are active or inert, the electron density difference section map around these two types of cations was calculated (Figure 6). The map clearly reveals the spherical region on Pb^{2+}, indicating the Pb^{2+}-$6s^2$ lone-pair electrons should be inert, whereas a lobe-like isosurface around the Se^{4+} cations confirms that the Se^{4+}-$4s^2$ lone pairs are stereoactive.

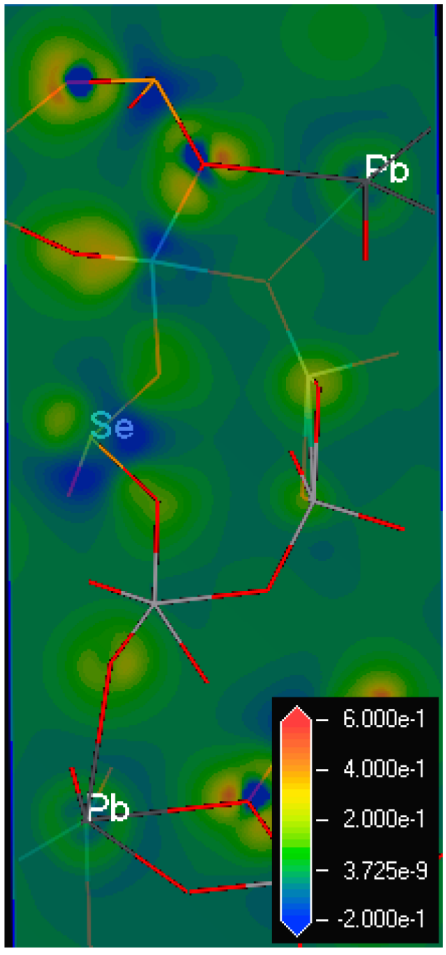

Figure 6. Electron density difference section map for the lead(II) and Se(IV) ions in $Pb_4V_6O_{16}(SeO_3)_3(H_2O)$.

CONCLUSIONS

In summary, we have successfully synthesized three new lead(II)−vanadium(V) selenites, namely, $Pb_4V_6O_{16}(SeO_3)_3(H_2O)$, $Pb_2VO_2(SeO_3)_2Cl$, and $PbVO_2(SeO_3)F$. Their structures feature three different vanadium(V) selenite anionic units: a 1D $[V_6O_{16}(SeO_3)_3]^{8-}$ branched chain, a 1D $[VO_2(SeO_3)_2]^{3-}$ chain, and a dinuclear $[V_2O_4(SeO_3)_2F_2]^{4-}$ cluster. Both $Pb_4V_6O_{16}(SeO_3)_3(H_2O)$ and $Pb_2VO_2(SeO_3)_2Cl$ are polar materials, and $Pb_4V_6O_{16}(SeO_3)_3(H_2O)$ displays a weak SHG signal of about 0.2 × KDP. Our future research efforts will be extended to the explorations of the alkali/alkaline earth metal-(d^0-TM)-Se^{4+}-oxyhalide systems in order to further understand the role halide anions play in these compounds.

ASSOCIATED CONTENT

Supporting Information

X-ray crystallographic files in CIF format, simulated and experimental XRD powder patterns, IR spectra, UV spectra, optical diffuse reflectance spectra, TGA, and DTA diagrams. This material is available free of charge via the Internet at http://pubs.acs.org.

AUTHOR INFORMATION

Corresponding Author

*E-mail: mjg@fjirsm.ac.cn.

Notes

The authors declare no competing financial interest.

ACKNOWLEDGMENTS

This work was supported by National Natural Science Foundation of China (Grants Nos. 21231006 and 91222108), NSF of Fujian Province (Grant No. 2011J05037), and State Key Laboratory of Structure Chemistry and Key Laboratory of Optoelectronic Materials Chemistry and Physics, CAS.

REFERENCES

(1) (a) Zhang, W.-L.; Cheng, W.-D.; Zhang, H.; Geng, L.; Lin, C.-S.; He, Z.-Z. *J. Am. Chem. Soc.* **2010**, *132*, 1508−1509. (b) Pan, S.; Smit, J. P.; Watkins, B.; Marvel, M. R.; Stern, C. L.; Poeppelmeier, K. R. *J. Am. Chem. Soc.* **2006**, *128*, 11631−11634. (c) Huang, Y.-Z.; Wu, L.-M.; Wu, X.-T.; Li, L.-H.; Chen, L.; Zhang, Y.-F. *J. Am. Chem. Soc.* **2010**, *132*, 12788−12789. (d) Harrison, W. T. A.; Dussack, L. L.; Jacobson, A. J. *Inorg. Chem.* **1994**, *33*, 6043−6049. (e) Harrison, W. T. A.; Dussack, L. L.; Jacobson, A. J. *J. Solid State Chem.* **1996**, *125*, 234−242. (f) Harrison, W. T. A.; Dussack, L. L.; Vogt, T.; Jacobson, A. J. *J. Solid State Chem.* **1995**, *120*, 112−120.

(2) (a) Halasyamani, P. S. *Chem. Mater.* **2004**, *16*, 3586−3592. (b) Johnston, M. G.; Harrison, W. T. A. *Eur. J. Inorg. Chem.* **2011**, 2967−2974. (c) Bang, S.-e.; Lee, D. W.; Ok, K. M. *Inorg. Chem.* **2014**, *53*, 4756−4762. (d) Kim, Y. H.; Lee, D. W.; Ok, K. M. *Inorg. Chem.* **2014**, *53*, 1250−1256.

(3) (a) Kim, S.-H.; Yeon, J.; Halasyamani, P. S. *Chem. Mater.* **2009**, *21*, 5335−5342. (b) Li, P.-X.; Hu, C.-L.; Xu, X.; Wang, R.-Y.; Sun, C.-F.; Mao, J.-G. *Inorg. Chem.* **2010**, *49*, 4599−4605. (c) Ok, K. M.; Halasyamani, P. S. *Angew. Chem., Int. Ed.* **2004**, *43*, 5489−5491. (d) Phanon, D.; Gautier-Luneau, I. *Angew. Chem., Int. Ed.* **2007**, *46*, 8488−8491.

(4) (a) Kim, J.-H.; Baek, J.; Halasyamani, P. S. *Chem. Mater.* **2007**, *19*, 5637−5641. (b) Ra, H. S.; Ok, K. M.; Halasyamani, P. S. *J. Am. Chem. Soc.* **2003**, *125*, 7764−7765. (c) Chi, E. O.; Ok, K. M.; Porter, Y.; Halasyamani, P. S. *Chem. Mater.* **2006**, *18*, 2070−2074. (d) Jiang, H.-L.; Huang, S.-P.; Fan, Y.; Mao, J.-G.; Cheng, W.-D. *Chem.−Eur. J.* **2008**, *14*, 1972−1981. (e) Kong, F.; Huang, S. P.; Sun, Z. M.; Mao, J.

G.; Cheng, W. D. *J. Am. Chem. Soc.* **2006**, *128*, 7750−7751. (f) Hu, T.; Qin, L.; Kong, F.; Zhou, Y.; Mao, J.-G. *Inorg. Chem.* **2009**, *48*, 2193−2199.
(5) (a) Porter, Y.; Bhuvanesh, N. S. P.; Halasyamani, P. S. *Inorg. Chem.* **2001**, *40*, 1172−1175. (b) Porter, Y.; Ok, K. M.; Bhuvanesh, N. S. P.; Halasyamani, P. S. *Chem. Mater.* **2001**, *13*, 1910−1915. (c) Kim, M. K.; Kim, S.-H.; Chang, H.-Y.; Halasyamani, P. S.; Ok, K. M. *Inorg. Chem.* **2010**, *49*, 7028−7.34.
(6) (a) Chang, H. Y.; Kim, S.-H.; Ok, K. M.; Halasyamani, P. S. *Chem. Mater.* **2009**, *21*, 1654−1662. (b) Chang, H. Y.; Kim, S. W.; Halasyamani, P. S. *Chem. Mater.* **2010**, *22*, 3241−3250. (c) Mao, J.-G.; Jiang, H.-L.; Kong, F. *Inorg. Chem.* **2008**, *47*, 8498−8510. (d) Ok, K. M.; Halasyamani, P. S.; Casanova, D.; Llunell, M.; Alemany, P.; Alvarez, S. *Chem. Mater.* **2006**, *18*, 3176−3183. (e) Zhang, S. Y.; Hu, C. L.; Sun, C. F.; Mao, J. G. *Inorg. Chem.* **2010**, *49*, 11627−11636. (f) Harrison, W. T. A.; Buttery, J. H. N. *Z. Anorg. Allg. Chem.* **2000**, *626*, 867−870.
(7) (a) Yeon, J.; Kim, S.-H.; Sau Doan, N.; Lee, H.; Halasyamani, P. S. *Inorg. Chem.* **2012**, *51*, 609−619. (b) Ok, K. M.; Bhuvanesh, N. S. P.; Halasyamani, P. S. *Inorg. Chem.* **2001**, *40*, 1978−1980. (c) Lee, E. P.; Song, S. Y.; Lee, D. W.; Ok, K. M. *Inorg. Chem.* **2013**, *52*, 4097−4103.
(8) (a) Li, P.-X.; Kong, F.; Hu, C.-L.; Zhao, N.; Mao, J.-G. *Inorg. Chem.* **2010**, *49*, 5943−5952. (b) Oh, S.-J.; Lee, D. W.; Ok, K. M. *Dalton Trans.* **2012**, *41*, 2995−3000. (c) Oh, S.-J.; Lee, D. W.; Ok, K. M. *Inorg. Chem.* **2012**, *51*, 5393−5399.
(9) (a) Becker, R.; Johnsson, M.; Kremer, R.; Lemmens, P. *Solid State Sci.* **2003**, *5*, 1411−1416. (b) Johnsson, M.; Törnroos, K. W.; Mila, F.; Millet, P. *Chem. Mater.* **2000**, *12*, 2853−2857. (c) Millet, P.; Bastide, B.; Pashchenko, V.; Gnatchenko, S.; Gapon, V.; Ksari, Y.; Stepanov, A. *J. Mater. Chem.* **2001**, *11*, 1152−1157. (d) Johnsson, M.; Törnroos, K. W.; Lemmens, P.; Millet, P. *Chem. Mater.* **2003**, *15*, 68−73. (e) Jiang, H.-L.; Mao, J.-G. *Inorg. Chem.* **2006**, *45*, 7593−7599.
(10) Cao, X.-L.; Hu, C.-L.; Xu, X.; Kong, F.; Mao, J.-G. *Chem. Commun.* **2013**, *49*, 9965−9967. (b) Li, H.; Wu, H.; Su, X.; Yu, H.; Pan, S.; Yang, Z.; Lu, Y.; Han, J.; Poeppelmeier, K. R. *J. Mater. Chem. C* **2014**, *2*, 1704−1710. (c) Wu, H.; Yu, H.; Yang, Z.; Hou, X.; Su, X.; Pan, S.; Poeppelmeier, K. R.; Rondinelli, J. M. *J. Am. Chem. Soc.* **2013**, *135*, 4215−4218.
(11) (a) *CrystalClear* Version 1.3.5; Rigaku Corp.: Woodlands, TX, 1999. (b) Sheldrick, G. M. *SHELXTL*, Version 5.1; Bruker-AXS: Madison, WI, 1998. (c) Spek, A. L. *PLATON*; Utrecht University: Utrecht, The Netherlands, 2001.
(12) Wendlandt, W. M.; Hecht, H. G. *Reflectance Spectroscopy*; Interscience: New York, 1966.
(13) Kurtz, S. K.; Perry, T. T. *J. Appl. Phys.* **1968**, *39*, 3798−3813.
(14) (a) Milman, V.; Winkler, B.; White, J. A.; Pickard, C. J.; Payne, M. C.; Akhmatskaya, E. V.; Nobes, R. H. *Int. J. Quantum Chem.* **2000**, *77*, 895−910. (b) Segall, M. D.; Lindan, P. J. D.; Probert, M. J.; Pickard, C. J.; Hasnip, P. J.; Clark, S. J.; Payne, M. C. *J. Phys.: Condens. Matt.* **2002**, *14*, 2717−2744.
(15) Perdew, J. P.; Burke, K.; Ernzerhof, M. *Phys. Rev. Lett.* **1996**, *77*, 3865−3868.
(16) Lin, J. S.; Qteish, A.; Payne, M. C.; Heine, V. *Phys. Rev. B* **1993**, *47*, 4174−4180.
(17) (a) Eaton, T.; Lin, J.; Cross, J. N.; Stritzinger, J. T.; Albrecht-Schmitt, T. E. *Chem. Commun.* **2014**, *50*, 3668−3670. (b) Sun, C.-F.; Hu, T.; Xu, X.; Mao, J. G. *Dalton Trans.* **2010**, *39*, 7960−7967.
(18) (a) Brese, N. E.; Okeeffe, M. *Acta Crystallogr., Sect. B: Struct. Sci.* **1991**, *47*, 192−197. (b) Brown, I. D.; Altermatt, D. *Acta Crystallogr., Sect. B: Struct. Sci.* **1985**, *41*, 240−244.
(19) Ninclaus, C.; Riou, D.; Ferey, G. *Chem. Commun.* **1997**, 851−852.
(20) (a) Ahn, H. S.; Lee, D. W.; Ok, K. M. *Inorg. Chem.* **2013**, *52*, 12726−12730. (b) Lee, D. W.; Ok, K. M. *Inorg. Chem.* **2013**, *52*, 10080−10086.
(21) Dutoit, D. C. M.; Schneider, M.; Fabrizioli, P.; Baiker, A. *Chem. Mater.* **1996**, *8*, 734−743.
(22) Luan, Z. H.; Kevan, L. *J. Phys. Chem. B* **1997**, *101*, 2020−2027.
(23) Choi, J.; Musfeldt, J. L.; Wang, Y. J.; Koo, H. J.; Whangbo, M. H.; Galy, J.; Millet, P. *Chem. Mater.* **2002**, *14*, 924−930.
(24) Ji, Z. X.; Ismail, M. N.; Callahan, D. M.; Warzywoda, J.; Sacco, A. *J. Photochem. Photobiol. A: Chem.* **2011**, *221*, 77−83.
(25) Sau Doan, N.; Halasyamani, P. S. *Inorg. Chem.* **2012**, *51*, 9529−9538.
(26) (a) Lee, D. W.; Oh, S.-J.; Halasyamani, P. S.; Ok, K. M. *Inorg. Chem.* **2011**, *50*, 4473−4480. (b) Izumi, H. K.; Kirsch, J. E.; Stern, C. L.; Poeppelmeier, K. R. *Inorg. Chem.* **2005**, *44*, 884−895.